

Stretched high-spin two-neutron-hole states in ^{206}Pb and ^{114}Sn via the (p, t) reaction at 168 MeV

E. Gerlic, J. Guillot, H. Langevin-Joliot, J. Van de Wiele, and S. Gales
Institut de Physique Nucléaire, 91406 Orsay CEDEX, France

G. Duhamel and G. Perrin
Institut des Sciences Nucleaire, 38026 Grenoble CEDEX, France

C. P. Massolo
Departemento de Fisica, Universidad de La Plata, 1900 La Plata, Argentina

M. Sakai
Institute for Nuclear Study, University of Tokyo, Tanashi-shi, 188 Tokyo, Japan
(Received 30 June 1988)

Two-neutron-hole excitations have been investigated via the (p, t) reaction at 168 MeV on ^{208}Pb and ^{116}Sn targets, up to ~ 25 and ~ 17 MeV excitation energy, respectively. The kinematic conditions strongly favor high L transfer values ($L \sim 10$ for Sn and $L \sim 13$ for Pb). High-spin stretched states are found to dominate the spectra with an even stronger enhancement for $J = [(l_1 + \frac{1}{2})(l_2 - \frac{1}{2})]_{J_{\max}}$ states. Angular distributions and standard local zero-range distorted-wave Born approximation analysis have been performed for ^{206}Pb . Such analysis has been extended to the ^{114}Sn data taken at two angles. The zero-range normalization constant D_0^2 is found to be significantly smaller than that usually adopted at low incident energy, $D_0^2 \sim 6$ instead of ~ 22 . The high-spin stretched states of the valence multiplets are distributed from 2.2 MeV up to 6.1 MeV in ^{206}Pb , whereas they are clustered between ~ 3.0 and 3.7 MeV in ^{114}Sn . New spectroscopic information gained for $J^\pi \geq 6$ levels or structures in ^{206}Pb and ^{114}Sn is discussed together with that of previous studies, especially the $(\alpha, ^6\text{He})$ results at high incident energy. Such comparisons show that configuration mixing is larger than predicted for the higher-energy transitions in ^{206}Pb . No significant concentration of valence plus deep hole states could be found in ^{206}Pb , whereas the previously known one valence plus one deep bump in ^{114}Sn exhibits a maximum at ~ 7.3 MeV here mainly attributed to the $(g_{7/2} + g_{9/2})_g^+$ state in agreement with the prediction of the quasiparticle phonon model.

I. INTRODUCTION

A large amount of experimental work has been devoted to the study of shell model single-particle modes in nuclei.¹ The two-nucleon transfer reactions may offer a different access to new "elementary" modes of excitation of the nuclear system.

In particular, the two-neutron hole excitations may be related to the general phenomena of valence and deep-hole states observed in one-neutron pickup reactions.^{1,2} The (p, t) reaction has been almost unexplored at high bombarding energies ($E_p > 60$ MeV). The few exceptions are one (p, t) experiment at 65 MeV incident energy on a ^{124}Sn (Ref. 3) target nucleus and two others studies at 80 MeV (Ref. 4) and 90 MeV (Ref. 5) on ^{208}Pb and $^{120, 122, 124}\text{Sn}$ target nuclei, respectively.

Most of the previous experiments have explored the low-lying and/or low-spin states. Only the (p, t) studies at 42 MeV (Refs. 6 and 7) and at 90 MeV (Ref. 5) incident energies on the tin isotopic chain were carried out to search for two-neutron strengths consisting of "one valence plus one deep" (1V+1D) or "two-deep" (2D)

quasihole configurations.

We have performed the (p, t) experiment at 168 MeV incident energy on several medium-heavy weight nuclei to gain information on higher-lying high-spin two-neutron hole states. At an incident proton energy of 168 MeV, strong enhancements of the reaction cross sections for large angular momentum transfers are kinematically expected up to rather high excitation energy. Among these high-spin states, the "stretched" states, where the spin of the transferred neutron pair is coupled to the maximum total spin J_{\max} with the condition

$$[(j_1 = l_1 + \frac{1}{2})(j_2 = l_2 - \frac{1}{2})]_{J_{\max}},$$

are predicted to be preferentially enhanced as a result of both large two-neutron transfer structure amplitudes⁸ and good matching conditions.

The present paper reports on a study of the (p, t) reaction on the ^{206}Pb target nucleus with a particular emphasis on the highest spin states resulting from the coupling of two valence hole orbitals (1V+1V) in ^{206}Pb . In addition, the residual excitation energy spectra have been investigated up to high excitation energy to look for

peaks or structures which could arise from high-spin (1V+1D) two-neutron-hole configurations.

A complementary study of the $^{116}\text{Sn}(p,t)^{114}\text{Sn}$ reaction has been undertaken to obtain new spectroscopic information on high-spin (1V+1V) and (1V+1D) two-neutron-hole strengths.

The results of the present work are compared with those deduced from the analysis of the $(\alpha, ^6\text{He})$ reaction at high incident energies on the same ^{116}Sn and ^{208}Pb target nuclei.^{9,10}

II. EXPERIMENTAL PROCEDURE AND DATA REDUCTION

The experiment was performed using the 168 MeV proton beam delivered by the K220 Orsay Synchrocyclotron. The magnetic analysis of the emerging tritons was possible due to the high magnetic rigidity of the "Montpellier" spectrometer. The detection system, at the focal plane of this spectrometer, has been described elsewhere.¹¹ The maximum allowed beam current on target was of ~ 250 nA. The thicknesses of the isotopically enriched targets were 20 and 50 mg/cm² for ^{208}Pb and 22 mg/cm² for ^{116}Sn . An energy resolution of typically 130 keV was achieved with the thin targets. Angular distributions were measured from 2 to 18 deg laboratory angles for the ^{208}Pb target while the spectra from the $^{116}\text{Sn}(p,t)^{114}\text{Sn}$ reaction were recorded at two angles (3.5 and 7 deg). The ^{206}Pb spectra were investigated up to 13 MeV at most angles and up to 25 MeV at two angles. The ^{114}Sn residual energy spectra were explored up to 17 MeV. In all cases, two or three different field settings of the spectrograph were necessary.

A typical spectrum from the reaction $^{208}\text{Pb}(p,t)^{206}\text{Pb}$ is displayed in Fig. 1. The excitation energies of the levels, groups or wider structures are listed in Table I together with the proposed spins and parities. The relevant data from previous (p,t) (Ref. 12) and $(\alpha, ^6\text{He})$ (Refs. 9 and 10) pickup studies are also listed for comparison.

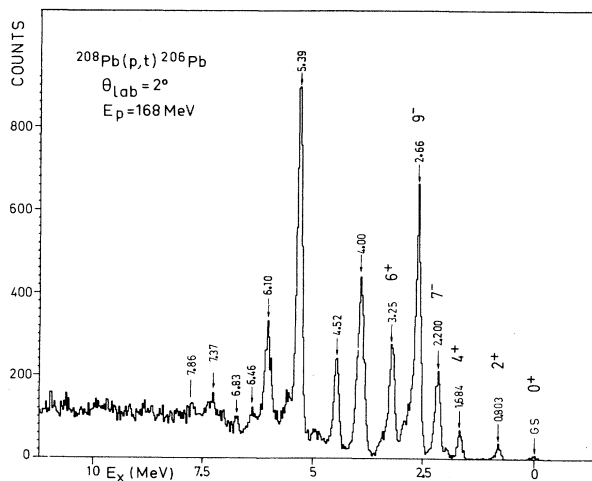


FIG. 1. Triton energy spectrum from the $^{208}\text{Pb}(p,t)^{206}\text{Pb}$ reaction at $E_p=168$ MeV and $\theta_{\text{lab}}=2^\circ$.

The well-known low-lying, low-spin states [$J^\pi \leq 4^+$, $E_x < 2.2$ MeV] are, as expected, very weakly excited. In contrast with the situation encountered at low incident energy,¹²⁻¹⁴ the strongest transitions occur between $E_x=2.2$ and 6.1 MeV. The 5.39 MeV peak is by far the most strongly excited state over the whole spectrum. The complex peak at about 4.0 MeV exhibits an unusually strong enhancement, especially at the largest angles. The excitation energies of the seven largest peaks correspond rather well to the location of the valence multiplets with $J_{\text{max}} \geq 6$, as expected from simple energy considerations.

These characteristic features of the ^{206}Pb spectrum demonstrate the high selectivity of the (p,t) reaction at high incident energy for large L transfers ($L \sim 13$ for the ^{208}Pb target). Interesting differences, which will be discussed later on, in the relative intensities of the peaks can be observed by comparing the present (p,t) spectrum with the $(\alpha, ^6\text{He})$ data obtained at 218 MeV incident energy, where the strongest excited states also show up in this same 2.2 to 6.1 MeV energy region. Beyond 6.7 MeV, where a clear minimum in the cross section is observed at all angles, the spectrum exhibits weak and broad structures at 6.46, 6.83, 7.37, and 7.86 MeV. They are superimposed on a flat continuum whose cross section increases slowly from 6.7 to ~ 14 MeV excitation energy.

The $^{116}\text{Sn}(p,t)^{114}\text{Sn}$ residual spectrum is presented in Fig. 2 together with the $(\alpha, ^6\text{He})$ spectrum obtained at 218 MeV incident energy.¹⁰ The relatively weak excitation of the first low-lying states ($0^+, 2^+, 4^+$) here again

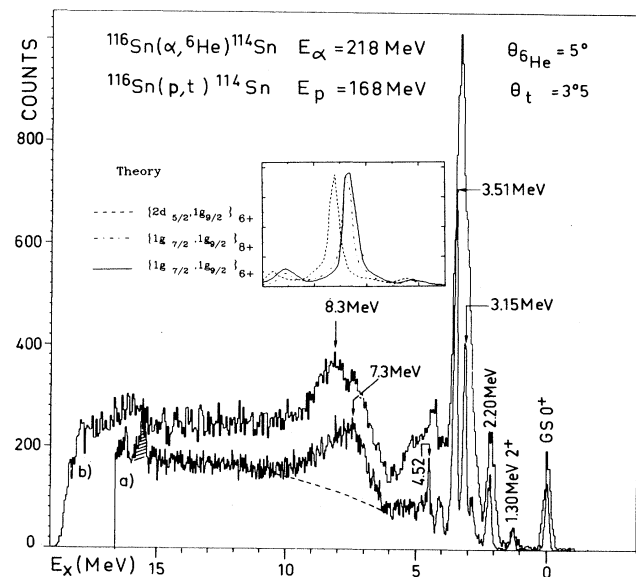


FIG. 2. ^{114}Sn excitation energy spectra. (a) $^{116}\text{Sn}(p,t)^{114}\text{Sn}$ reaction at $E_p=168$ MeV and $\theta_{\text{lab}}=3.5^\circ$. The dashed line indicates the shape of the assumed subtracted background in the bump region. (b) $^{116}\text{Sn}(\alpha, ^6\text{He})^{114}\text{Sn}$ reaction at $E_\alpha=218$ MeV and $\theta_{\text{lab}}=5^\circ$ (taken from Ref. 10). The inset corresponds to calculated neutron 2-qp strength distribution for the (1V+1D) structure as reported in Ref. 29.

TABLE I. $^{208}\text{Pb}(p,t)^{206}\text{Pb}$ reaction data at 168 MeV and comparison with previous works.

(p,t) 168 MeV present work		(p,t) 52 MeV (Ref. 12)		$(\alpha, ^6\text{He})$ 218 MeV (Ref. 10)		$(\alpha, ^6\text{He})$ 109 MeV (Ref. 9)	
E_x (MeV)	J^π	E_x (MeV)	J^π	E_x (MeV)	J^π	E_x (MeV)	J^π
(0)	(0 ⁺)	0.0	0 ⁺	0.0	(0 ⁺)	0.0	0 ⁺
0.80	2 ⁺	0.80	2 ⁺	0.80	2 ⁺	0.80	2 ⁺
		1.17	0 ⁺			1.34	3 ⁺
		1.46	2 ⁺			1.47	2 ⁺
1.68	4 ⁺	1.69	4 ⁺	1.7	4 ⁺	1.68	4 ⁺
						1.78	2 ⁺
(2.00)	(4 ⁺)	1.99	4 ⁺			2.00	4 ⁺
						2.15	2 ⁺
2.20	7 ⁻	2.19	7 ⁻	2.20	7 ⁻	2.20	7 ⁻
		2.40	2 ⁺			2.32	0 ⁺
						2.42	2 ⁺
2.66	9 ⁻	2.66	9 ⁻	2.65	9 ⁻	2.66	9 ⁻
		2.79	5 ⁻			2.78	5 ⁻
						2.87	7 ⁻
2.91 ^a	(7 ⁻ +4 ⁺)	2.93	4 ⁺	2.90 ^a	(4 ⁺)	2.93	4 ⁺
						3.01	5 ⁻
						3.12	3 ⁺
3.25	6 ⁺	3.26	6 ⁺	3.25	6 ⁺	3.26	6 ⁺
3.49	(4 ⁺)(5 ⁻)	3.54	5 ⁻				
		3.77	2 ⁺			3.77	2 ⁺
4.00 ^a ±0.04	12 ⁺ +10 ⁺ +(8 ⁺)	3.96	9 ⁻ ,8 ⁺	3.95 ^a	6 ⁺ (+4 ⁺)	3.96	4 ⁺
		4.16	3 ⁻				
4.52 ^a ±0.04	9 ⁻ +7 ⁻	4.56	7 ⁻	4.47 ^a ±0.04	(7 ⁻) or (6 ⁺)	4.52	(6 ⁺)
				4.77±0.05			
(5.00±0.05)		4.90	7 ⁻				
		5.10	7 ⁻	(5.25±0.06)		5.36	(6 ⁺)
5.39±0.035	11 ⁻ (+9 ⁻)	5.41	11 ⁻	5.38 ^a ±0.06	9 ⁻ (+11 ⁻)	5.41	11 ⁻
5.61±0.06	(9 ⁻)	5.70	(9 ⁻ +3 ⁻) or 4 ⁺	(5.6±0.065)			
		5.8	8 ⁺				
6.10 ^a ±0.04	8 ⁺ +(9 ⁻)	6.2	9 ⁻	6.1±0.07	8 ⁺	6.10	(9 ⁻)
						6.13	(8 ⁺)
6.46±0.06		6.5	6 ⁺	6.4±0.08			
6.83±0.06							
7.37±0.07	> 8			7.35±0.08	≥ 7		
7.86±0.08				7.90 ^a ±0.09			

^aComplex peak.

reflects the high angular momentum selectivity of both processes [$L \sim 10$ for the (p,t) reaction on the ^{116}Sn target]. The doublet around 3.4 MeV and the gross structure located at 7.3 MeV clearly dominate the entire spectrum. Similar features are observable in the $(\alpha, ^6\text{He})$ data, except that the main peak at 3.4 MeV cannot be resolved and the bump is found to have a maximum cross section around 8.3 MeV rather than 7.3 MeV as it is shown in Fig. 2. In addition, the high-energy tail of the bump in the (p,t) spectrum has a much more asymmetric shape than in the $(\alpha, ^6\text{He})$ case. These differences will be discussed in Sec. IV. Above the gross structure, no other pronounced enhancement is found up to 17 MeV excitation energy. The continuum cross section has a behavior similar to the one already mentioned in the case of the ^{208}Pb target. The bump cross sections at 3.5° and 7.0° lab angles have been deduced after subtraction of a “background” as indicated by the dashed line displayed in Fig. 2.

III. DWBA ANALYSIS

The angular distributions of the strongest excited levels in ^{206}Pb have been analyzed in the framework of a standard local zero-range distorted-wave Born approximation (LZR-DWBA), using the code DWUCK4. All calculations were carried out with microscopic form factors built up from the single-neutron form factors generated in a standard Woods-Saxon potential adjusted to give a binding energy equal to one half of the two-neutron separation energy. A standard geometry ($r=1.25$ fm, $a=0.65$ fm) was used for each neutron bound state form factor. Various sets of proton and triton optical potential parameters taken from the literature, were employed in the analysis. All sets are found to reproduce rather well the relative cross sections at forward angles for the known stretched states $(p_{1/2} \times i_{13/2})_{7-}$ at $E_x=2.2$ MeV, $(f_{5/2} \times i_{13/2})_{9-}$ at $E_x=2.66$ MeV, and $(f_{5/2} \times f_{7/2})_{6+}$ at $E_x=3.25$ MeV. This was found to be also the case for the peaks at

$E_x=4.0$, 5.39, and 6.1 MeV assuming that they mainly contain the stretched states with the following configurations: $(i_{13/2} \times i_{13/2})_{12^+}$, $(i_{13/2} \times h_{9/2})_{11^-}$, and $(f_{7/2} \times h_{9/2})_{8^+}$, respectively (see Table III). The relative magnitude of these cross sections, assuming pure two-neutron-hole configurations, demonstrates the preferential excitation of the stretched states with total spin J_{\max} such as

$$J = [(l_1 + \frac{1}{2}) \times (l_2 - \frac{1}{2})]_{J_{\max}}$$

as compared with the other kinematically favored transitions with a total spin J_{\max} resulting from different couplings such as

$$J_{\max} = (l_1 \pm \frac{1}{2})(l_2 \pm \frac{1}{2})$$

or $J_{\max} = (j)^{-2}$. Also high spins with $J = J_{\max-1}, J_{\max-2}$ are, in any couplings, much less favored. On the other hand, the shapes of the calculated angular distributions were found to be strongly sensitive to the potential parameters of the exit channel. The adopted optical potentials are listed in Table II. The proton parameters of Djalali *et al.*¹⁵ were used to describe the entrance channel, whereas the so-called "volume-deep" ³He optical potential of Djaloeis *et al.*¹⁶ was selected for the exit channel.

The experimental and calculated (DWBA) angular distributions of the seven strong peaks are displayed in Fig. 3. The agreement between the DWBA curves and the experimental data is satisfactory for $L \geq 6$ transfers. However, these LZR-DWBA calculations do not reproduce the shapes of the angular distributions in the case of strong mismatched transitions ($L < 6$).

For the ¹¹⁶Sn(*p,t*)¹¹⁴Sn reaction, the LZR-DWBA cross sections were calculated using the same set of optical potential parameters which also proved quite successful for describing the (*p,t*) reaction at 168 MeV on Zr nuclei.¹⁷

The experimental (*p,t*) cross section $(d\sigma/d\Omega)_{\text{expt}}$ for a single pure two-neutron-hole configuration $[(n_1, l_1, j_1)(n_2, l_2, j_2)]_{LJ}$ is related to the LZR-DWBA cross section σ_{DW} by the expression

$$(d\sigma/d\Omega)_{\text{expt}} = NC^2 S \frac{\sigma_{DW}}{2J+1} \epsilon, \quad (3.1)$$

where

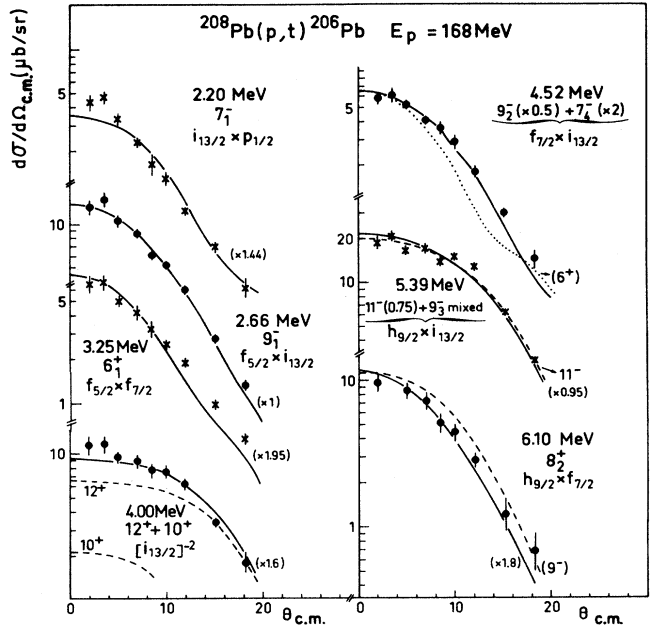


FIG. 3. Typical angular distributions for the ²⁰⁸Pb(*p,t*)²⁰⁶Pb reaction at 168 MeV. The curves are LZR-DWBA predictions. Solid lines are the $J=L$ adopted fits. Relevant configurations are indicated. The smaller numbers into brackets reflect the renormalization factor ϵ_r of Table III used to adjust the experimental data with the DWBA predictions assuming one pure configuration. "9₃⁻ mixed" stands for the proposed admixture in the wave function of the 9₃⁻ level (see the text and Fig. 4).

$$N = D_0^2 \left[\pi \frac{\Delta^2}{2} \right]^{3/2} (\Delta'/\Delta)^6. \quad (3.2)$$

In Eq. (3.1), the C^2 coefficient is the isospin coupling constant and is equal to unity for the (*p,t*) reaction. The S factor represents the two-neutron spectroscopic factor and is set equal to $(2J+1)$ for neutron closed-shell nuclei (²⁰⁸Pb). In the case of partially filled subshells (¹¹⁶Sn), the S factor is equal to $(2J+1)V_{j_1}^2 V_{j_2}^2$, where $V_{j_1}^2$ and $V_{j_2}^2$ are the occupation probabilities for each neutron (j_1, j_2). The ϵ parameter characterizes the ratio of experimental to DWBA cross sections and is usually called the enhancement factor. It reflects the degree of deviation from a shell model prediction based on a pure

TABLE II. Optical potential parameters used in the distorted-wave calculations.

Particles	V_r (MeV)	r_0 (fm)	a_r (fm)	W_I (MeV)	r_I (fm)	a_I (fm)	U_{s0}^d (MeV)	W_{s0}^d (MeV)	r_{s0} (fm)	a_{s0} (fm)	r_c (fm)
Proton ^a	19.65	1.223	0.736	18.13	1.213	0.829	8.26	3.012	1.113	0.558	
Triton ^b	180.0	1.092	0.902	17.8	1.538	0.757					
<i>n,p</i>	adjusted ^c	1.25	0.75				$\lambda=25$				

^aReference 15.

^bReference 16.

^cAdjusted to reproduce half the binding energy of the *n,p* pair.

^dFactor 4 included.

configuration and measures the relative strengths of the various (p,t) transitions.

In Eq. (3.2), D_0^2 is the zero-range normalization constant (ZRNC), Δ is the rms radius of the triton and is usually set to 1.7 fm. Δ' is taken here equal to Δ since the two-body interaction is assumed of long-range type. Therefore, using Eq. (3.2): $N=9.7 D_0^2$.

At this stage we would like to stress that in the literature, scattered values of the ZRNC D_0^2 are reported. The analysis of the (p,t) reaction, on various medium-heavy weight targets and at incident energies ranging from 25 to 90 MeV (Refs. 18, 3, and 4), seems to reveal an energy dependence of D_0^2 . The empirical value of D_0^2 is believed to depend strongly on the appropriate choice for the state of reference (pure two-neutron-hole state), since the (p,t) cross sections are known to be very sensitive to configuration mixing. Therefore, we emphasize that a good determination of the ZRNC D_0^2 which has never been attempted at such a high incident energy, requires a reference state with one pure configuration in a closed-shell nucleus. This goal is better achieved with high-spin states at low excitation energies, since the number of configurations is severely restricted. Such requirements are believed to be fulfilled in the present study of the $^{208}\text{Pb}(p,t)^{206}\text{Pb}$ reaction at 168 MeV incident energy.

In a first step, the known low-lying 9^- level at 2.66 MeV with the quasipure $(f_{5/2} \times i_{13/2})$ configuration^{12,19} has been used as a reference state ($\epsilon_{9^-} = 1$). A ZRNC D_0^2 value of 4.2 in ($10^4 \text{fm}^3 \text{MeV}^2$ units) is then deduced. This result has to be compared with the D_0^2 value of 22, commonly adopted for (p,t) reactions at lower incident energies ($E \leq 60$ MeV). A similar analysis of the reaction $^{90,92}\text{Zr}(p,t)$ at 168 MeV incident energy also yields¹⁷ a small ZRNC ($D_0^2 \sim 2.3$). In any case, for the $^{208}\text{Pb}(p,t)$

reaction, if other reasonable sets of proton and triton potential parameters are used, then under the same assumptions the values of D_0^2 obtained range between ~ 3 and ~ 7 , and the general conclusions about the relative intensities of the main transitions are not affected.

At this stage it is worthwhile to notice that the two-neutron-hole states may also be fragmented via their coupling to surface vibrations in addition to the configuration mixing. This same process has previously been demonstrated to be responsible for the one hole fragmentation observed via one-nucleon-pickup reactions.^{1,2} For example, the first $\frac{13}{2}^+$ and $\frac{9}{2}^-$ levels, respectively, at $E_x = 1.63$ MeV and $E_x = 3.42$ MeV in ^{207}Pb , have been shown to exhaust only 72% and 50% of the corresponding $i_{13/2}$ and $h_{9/2}$ hole strengths. Considering such one-quasihole levels as the building blocks of two-neutron quasihole states implies that the calculated cross section σ_{DW} in Eq. (3.1) is replaced by $\sigma_{DW} \times R$, thus increasing the extracted N value. Specifically, the reduction factor R (quoted in Table III for each two-neutron-hole configuration) is set as the product of the $1qh$ probabilities measured in the two related lowest levels of ^{207}Pb .^{20,21} Then, using the sum rule obtained for the 9^- states as discussed later, a more realistic D_0^2 value is deduced, namely $D_0^2 = 6.6$. A maximum value of $D_0^2 \sim 8.3$ could be obtained, if one uses a global sum rule, taking into account the main transitions with spins $J \geq 6$ located between 2.2 and 6.1 MeV excitation energies.

Therefore, the present LZR-DWBA analysis of the (p,t) reaction at 168 MeV incident energy leads to a ZRNC D_0^2 much smaller than the one usually deduced from previous lower-energy (p,t) studies. The decreasing value of D_0^2 with higher incident energy has been already pointed out by the authors of Refs. 3 and 18.

TABLE III. The $^{208}\text{Pb}(p,t)^{206}\text{Pb}$, reaction at 168 MeV: Analysis of the main observed transitions.

E_x (MeV)	J^π	ϵ_r^b	R^c	Main configuration ^d	$E_{x_{\text{th}}}^d$ (keV)	$E_{x_{\text{th}}} - E_{x_{\text{exp}}}$ (keV)
2.20	7_1^-	1.44	0.72	$0.96(p_{1/2} * i_{13/2})$	2.48	+280
2.66	9_1^-	1	0.72	$0.99(f_{5/2} * i_{13/2})$	2.93	+270
3.25	6_1^+	1.95	0.88	$0.95(f_{5/2} * f_{7/2})$	3.36	+210
4.00 ^a	12_1^+	1.60	0.52	$1.00(i_{13/2})^{-2}$	4.34	+340
	if 10_1^+	5.60		$1.00(i_{13/2})^{-2}$	4.28	+280
	if (8_1^+)	(~ 24)		$0.99(i_{13/2})^{-2}$	4.22	+220
4.52 ^a	9_2^-	1.20	0.63	$0.99(f_{7/2} * i_{13/2})$	4.99	+490
	if $+7_4^-$	4.20	0.63	$0.99(f_{7/2} * i_{13/2})$	4.93	+430
5.39	11_1^-	0.95	0.36	$1.00(h_{9/2} * i_{13/2})$	5.65	+300
	(if 9_3^-)	(~ 15)	0.36	$0.997(h_{9/2} * i_{13/2})$	6.04	+660
6.10 ^a	$8_2^+ (+9^-)$	1.8	0.44	$0.996(h_{9/2} * f_{7/2})$	6.55	+450

^aDoublet peak.

^bEnhancement factor relative to the 9_1^- state taken as the reference; assuming one pure configuration and no fragmentation (see the text).

^cReduction factor resulting from the fragmentation of each involved single hole strength and by which the σ_{DWBA} should be multiplied in Eq. (3.1). (See the text, Secs. III and IV).

^dKuo and Herling (Ref. 19) approximation 2.

IV. RESULTS AND DISCUSSION

A. Two-neutron-hole states in ^{206}Pb

The spectroscopic properties of the two-neutron-hole states, selectively populated in the present experiment, are summarized in Table III. The main configuration, the spectroscopic amplitude, and excitation energy as predicted by Kuo-Herling¹⁹ are indicated for each state of interest. One may notice that all strongly excited states have a predicted quasipure two-neutron-hole configuration. More recent calculations¹² lead to the same conclusion which reinforces the choice of the $E_x=2.66$ MeV $J^\pi=9_1^-$ state as a reference one ($\epsilon_{9_1^-}=1$). The relative enhancement factors ϵ_r , given in Table III, assuming for each level one pure two-neutron-hole configuration is used as the first step of the discussion. These ϵ_r values range from 0.95 to 1.95 if only the “stretched” high-spin states are considered. If, for a given state, lower-spin assignments are attempted, unreasonably large values of ϵ_r ($\epsilon_r \gtrsim 4$) are obtained (see Table III).

In the following we shall first only discuss the main excited levels, since the weaker transitions belonging either to unfavored configurations ($J_{\text{max}} < 6$) or to small fragments of higher-spin states are outside the range of validity of the attempted analysis. Then we shall discuss the measured and calculated sum rules and the fragmentation of the two-quasiparticle (2-qp) strengths induced by the coupling to surface vibrations as mentioned above. This process may affect high-spin as well as lower-spin states, especially at excitation energies higher than ~ 4 MeV.

1. Low-lying levels at $E_x=2.2$, 2.66 , and 3.25 MeV

These states are strongly populated in the four reactions quoted in Table I. Their spins, parities, and main configurations are well established (see Table III). The predicted excitation energies¹⁹ are systematically higher than the experimental ones by about 250 keV. The relative enhancement factors obtained for the 7^- and 6^+ states are found to be somewhat larger than 1. One can notice (Table III) that these two states involve the less pure predicted main configuration, as can be expected with such intermediate spin values. A more refined analysis, taking into account the most significant configuration amplitudes in the Kuo-Herling corresponding wave functions, does not change significantly the shape of the angular distributions but the absolute cross sections. Smaller ϵ_r values are deduced, thus improving the agreement between theoretical and experimental cross sections (typically ϵ_r tends to ~ 1.0 instead of ~ 1.44 and to ~ 1.5 instead of ~ 1.9 for the 7_1^- and 6_1^+ states, respectively).

2. The 4.00 MeV peak

The angular distribution of this complex peak exhibits an unambiguous $L \geq 10$ pattern. The levels strongly populated through the (p,t) reaction at 168 MeV thus differ from the lower-spin states observed at the same excita-

tion energy in the $(\alpha, ^6\text{He})$ reaction at 109 MeV,⁹ at 218 MeV (Ref. 10) and in the (p,t) reaction at 52 MeV (Ref. 12) (see Table I). Both the absolute cross section and the shape of the angular distribution are well reproduced by assuming the excitation of at least the two highest spin members of the $(i_{13/2})^{-2}$ multiplet, the stretched 12^+ state carrying about 65% of the peak cross section (see Fig. 3 and Table III). These 12^+ and 10^+ members of the $(i_{13/2})^{-2}$ multiplet have been clearly identified up to now via in beam γ -spectroscopy experiments²² at $E_x=4.03$ and $E_x=3.96$ MeV, respectively. It is worthwhile to point out that the unfavored nature of the $(jj)_{J_{\text{max}}}$ two-neutron-hole configuration is overcome in the present work by the matching conditions which enhance such large $L=12$ transfers. Even better agreement with the experimental differential cross sections at forward angles can be obtained by adding small contributions arising from the close 8_1^+ and 6_2^+ states, unresolved in this study and belonging to the same multiplet (see Table I).

3. The 4.52 MeV peak

The shape of the angular distribution is well reproduced by angular momentum transfers ranging from $L=7$ to $L=9$. Previous (p,t) and $(\alpha, ^6\text{He})$ experiments have assigned a spin and parity $J^\pi=7^-$ (Refs. 12 and 10) and/or possibly $J^\pi=6^+$ (Refs. 10 and 9) to this complex peak at $E_x=4.52$ MeV. It is reasonable to assume that the peak contains the $J^\pi=7_4^-$ member of the $(i_{13/2} \times f_{7/2})$ multiplet from simple excitation energy considerations. The $J^\pi=9_2^-$ stretched member of this less favored multiplet is expected to lie nearby. As shown in Table III, the enhancement factor ϵ_r would favor a $J^\pi=9_2^-$ assignment. But on the other hand, it is surprising that this 9_2^- level was not identified in the study of the $(\alpha, ^6\text{He})$ reaction at 218 MeV (Ref. 10) which strongly favors $L=9$ transfer, nor in the (p,t) study at 52 MeV (Ref. 12) performed with much better energy resolution. After a close examination of all these results, we conclude that, despite the proposed quasipure character of the 9_2^- state,^{12,19} small ($\sim 5\%$) configuration mixing with the $(i_{13/2} \times h_{9/2})_{J_{\text{max}-2}}$ and the much favored $(f_{5/2} \times i_{13/2})_{J_{\text{max}}}$ amplitudes may induce destructive interference effects on the cross section of the 9_2^- component. On the other hand, constructive configuration mixing accounts for the population of the 7_4^- level. With these assumptions, the two members 9_2^- and 7_4^- are excited with comparable cross sections in the present experiment while the 7_4^- level becomes dominant in the previous (p,t) study at 52 MeV and in the $(\alpha, ^6\text{He})$ spectra at 218 MeV.

4. The 5.39 MeV peak

The present work gives the first clear evidence for the identification of the $(i_{13/2} \times h_{9/2})_{11^-}$ stretched state in ^{206}Pb . The angular distribution is characteristic of a $L=11$ transition as shown in Fig. 3. From energy considerations, the 11^- state is expected around 5.4 MeV, and theoretical calculations¹⁹ confirm this crude estimate.

This level was tentatively observed as a weak peak in previous studies.^{10,12-14} However, in the (α , ^6He) reaction at 218 MeV (Ref. 10) the complex peak observed at 5.38 MeV was proven to be clearly populated through a $L=9$ transfer. This level was first proposed to be the $J^\pi=9_3^-$ ($J_{\text{max}}-2$) member of the same ($i_{13/2} \times h_{9/2}$) multiplet (thus of unfavored character). That assignment, as noted in Ref. 10, did not exclude the weak contribution of the 11^- level.

The angular distributions of this close doublet measured in both reactions, as shown in Fig. 4, illustrate the competition between the two level contributions and the need to introduce a small (5% to 10% in weight) but larger than predicted^{12,19} constructive configuration mixing for the 9_3^- state, to explain the measured cross sections in both experiments (see Fig. 4). This strongly constructive interference would be the counterpart of the destructive interference proposed for the 9_2^- level. Then it follows that the (p,t) reaction at 168 MeV enhances mainly the 11^- component while the (α , ^6He) process at 218 MeV preferentially populates the 9_3^- component of this unresolved doublet arising from the same ($i_{13/2} \times h_{9/2}$) multiplet. From the results of the two experiments, an enhancement factor of $\epsilon_r \sim 0.75$ is deduced for the 11^- state, in fair agreement with the known large fragmentation of the $h_{9/2}$ hole compared with that of the $f_{5/2}$ hole strength in ^{207}Pb (see Table III).

5. The 6.10 MeV peak

The angular distribution of this complex peak is best reproduced by a $L=8$ transfer (see Fig. 3). This result

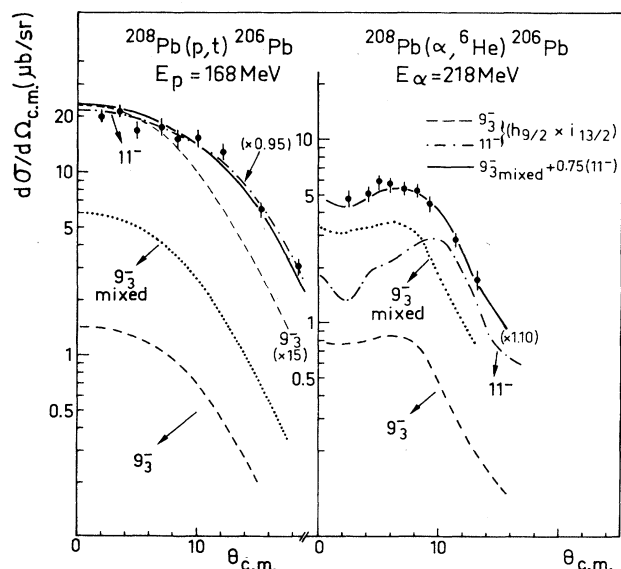


FIG. 4. Angular distribution measured for the 5.3 MeV (11^-+9^-) doublet from the (p,t) and (α , ^6He) reactions at 168 MeV and 218 MeV, respectively. The LZR-DWBA fits (full curves) are obtained assuming in both cases the same configuration mixing for the 9_3^- level, i.e., $\sim 90\%$ ($i_{13/2} \times h_{9/2}$) + 10% ($i_{13/2} \times f_{5/2}, f_{7/2}$), and 75% ($i_{13/2} \times h_{9/2}$) 11^- .

confirms the spin and parity assignment $J^\pi=8_2^+$ for the stretched member of the ($f_{7/2} \times h_{9/2}$) multiplet.¹⁰ The relatively large ϵ_r value can be accounted for by adding contributions to the peak cross section arising from higher spin ($J>8$) components in agreement with previous works^{9,12} and as discussed below.

6. The valence-valence ($1V+1V$) two-neutron-hole strength sum rule

At high incident energy, the (p,t) DWBA cross sections are nearly Q independent. By adding up cross sections of the different levels with the same spin and parity one obtains a quantity which is rather insensitive to configuration mixing, thus allowing a consistent check of the present analysis. This sum-rule analysis was attempted for the highest spin states ($J \geq 6$) strongly excited in this experiment.

The ratio of the experimental and DWBA summed cross sections are reported in Table IV for the ($12^+, 10^+$), 11^- and 9^- states identified below 6.1 MeV and for the sum of all the transitions with $J \geq 6$ located between $E_x=2.2$ and 6.1 MeV.

First we have assumed that the measured cross sections exhaust the full corresponding two-neutron-hole strength [deduced N value from Eq. (3.1) in Table IV], which would imply that coupling with surface collective vibrations is negligible. Since the model space contains all the relevant $(2\nu)^{-2}$ transitions, N should be constant and independent of J , if this assumption of no fragmentation is valid. Then the N value from the 11^- state appears significantly smaller than for the other states, which would reveal a particular fragmentation of this level. In a more realistic approach, we have taken into account the fragmentation of the related single hole strengths induced by the coupling with collective states. Namely, the DWBA cross sections have been reduced by the R factor defined in Sec. III and given in Table III. If the two-neutron-hole fragmentation is correctly estimated by these R factors, then the new N' values also are expected to be constant. The results of this sum-rule analysis are listed in Table IV. The slight difference observed between the N' values of the 9^- sum rule and those of the 11^- and $12^+, 10^+$ states may tentatively be related to the fact that both involved single hole strengths in these last high-spin states are known to be strongly fragmented, namely the $i_{13/2}$ and the $h_{9/2}$ strengths, whereas this is

TABLE IV. Sum-rule analysis of the $^{208}\text{Pb}(p,t)^{206}\text{Pb}$ reaction at 168 MeV and normalization factors deduced from Eq. (3.1) for the high-spin state transitions from $E_x=2.2$ MeV to 6.1 MeV in ^{206}Pb .

J^π	$\Sigma 9^-$	11^-	$12^+, 10^+$	$\Sigma J \geq 6$
N^b	43	30	41	42
$N^{c\prime}$	64 ^a	83	80	81

^aAdopted value. Then $D_0^2 \sim 6.6$ [from Eq. (3.2)], see the text.

^bWithout taking into account the single-particle fragmentation.

^cTaking into account the related single hole fragmentation (Refs. 20 and 21): the predicted σ_{DW} cross sections are reduced by R factors of Table III. (See the text.)

not the case of the $f_{5/2}$ hole in the $(f_{5/2} \times i_{13/2})$ configuration which yields the dominant contribution to the 9^- sum rule. It seems reasonable to assume that the 9^- sum rule governed by the 9_1^- level at 2.65 MeV is better estimated by our crude model of the R factor than those of the high-spin states located at higher excitation energies. Thus $N' \simeq 64$ is adopted (Table III) leading to the ZRNC $D_0^2 \simeq 6.6$. As a result we would conclude that the 11^- and 12^+ state fragmentation is somewhat overestimated by the R factor. The $J \geq 6$ 2-qp levels would thus exhaust typically between $\sim 90\%$ (6^+) and 47% (11^-) of their valence-valence strengths, and globally $\sim 66\%$ of the total $J^\pi \geq 6$ (1V+1V) strength (as can be deduced from Table IV).

The (1V+1V) missing strength would be shared among many (phonon+2-qp) states. The (2-qp \times 3 $^-$) states built with the ^{208}Pb high-spin 2-qp levels and the strong octupole vibration at $E_x = 2.6$ MeV would extend from ~ 4.8 MeV up to 8.7 MeV from simple energy considerations, and the so-called intermediate coupling region may extend up to ~ 10.5 MeV if one extrapolates the results obtained with the $^{207}\text{Pb}(^3\text{He},\alpha)^{206}\text{Pb}$ reaction²⁰ on intermediate coupling states. It is worthwhile to notice that this region is expected to already overlap with the higher energy strong transitions such as $J^\pi = 11^-$ and $J^\pi = 8^+$ at $E_x = 5.39$ MeV and 6.1 MeV, respectively. A collective 9^- level has been proposed at $E_x = 6.18$ MeV.⁹ These remarks are in agreement with the fact that the stretched states observed beyond $E_x \sim 4$ MeV in the present experiment have less and less pure configurations than predicted^{12,19} and larger deviations from the theoretical excitation energies (see Table III).

7. The higher excitation energy region in ^{206}Pb beyond 6.7 MeV

The ^{206}Pb excitation energy spectrum exhibits indeed an increasing density of states with significant cross sections beyond 6.7 MeV.

The angular distributions of the raw energy slices (up to ~ 12 MeV) are rather similar and characteristic of a $L \geq 9$ transfer. Then the weak structures riding over the continuum at $E_x = 7.37$ MeV and 7.86 MeV may contain some amount of the 11^- (or 12^+ and 9^-) missing strengths. The estimated 35% missing cross sections in the first $J \geq 6$ 2-qp fragments would thus mainly contribute to the continuum both below $E_x = 6.7$ MeV and mostly beyond that energy ($\sim 25\%$). It is encouraging that the total cross section measured from $E_x = 6.7$ MeV up to ~ 10.5 MeV is compatible with this estimation, taking into account the contributions of an underlying physical background and of the overlapping (1V+1D) states expected beyond $E_x = 8$ MeV.

Up to 25 MeV excitation energy, the recorded spectra give no indication of a significant enhancement of cross sections corresponding to the one valence plus one deep two-neutron-hole strength. A significant concentration of the high-spin states based on $i_{13/2}$ and $h_{9/2}$ valence hole and $h_{11/2}$ deep hole orbitals is expected to lie between ~ 8 and 13 MeV. Therefore, from ~ 7.5 to ~ 9.5 MeV, the (1 ph +2-qp) intermediate coupling region and

the (1V+1D) region strongly overlap. The (1V+1D) strength might be highly damped over a large excitation energy range due to the known spreading of the $h_{11/2}$ deep-hole strength.^{20,21} In one-neutron-pickup experiments, only 53% of the $h_{11/2}$ deep-hole strength was found between 6.6 and 9.8 MeV in ^{207}Pb . In addition, the valence orbitals ($i_{13/2}$ and/or $h_{9/2}$) are themselves significantly fragmented.^{20,21}

B. Two-neutron-hole states in ^{114}Sn

The main characteristics of the observed levels are summarized in Table V. In the following we will discuss the results obtained for the (1V+1V) and the (1V+1D) two-neutron-hole states in ^{114}Sn .

1. The valence-valence two-neutron-hole region ($2.5 < E_x < 3.8$ MeV)

This excitation energy range few investigated in ^{114}Sn up to now corresponds to the neutron 2-qp valence hole states as predicted from energy and pairing considerations. The minimum energy for 2-qp states is about 2.4 MeV. The valence single-hole strength is distributed among five subshells, namely, $2d_{5/2}$, $1g_{7/2}$, $2d_{3/2}$, $3s_{1/2}$, and $1h_{11/2}$. Their corresponding occupation probabilities V_j^2 are measured in one-neutron pickup experiments.²³ Almost the full hole strength is concentrated in the first level of each spin.

The (p,t) reaction at high incident energy populates selectively a cluster of states around 3.4 MeV in a similar way to the ($\alpha,^6\text{He}$) reaction at 218 MeV (Ref. 10) (see Fig. 2). From the ($\alpha,^6\text{He}$) study a typical $L=6$ angular distribution has been obtained for the complex peak at 3.4 MeV, in agreement with the previously identified 6^+ states at $E_x = 3.148$ and 3.472 MeV.²⁴ This dominant $J^\pi = 6^+$ assignment is consistent with the favored $(g_{7/2} \times d_{5/2})$, (1V+1V) stretched state rather than with the $(g_{7/2})^{-2}$ configuration.

In the present (p,t) study, two levels at 3.15 and 3.51 MeV are excited (Fig. 1). The ratio of their experimental cross sections measured at 3.5° and 7° laboratory angles is compared with the corresponding DWBA ratio to determine the most probable transfer values ($L \pm 1$) (expected ratios being typically ~ 1.4 for $L \sim 6$ and ~ 1.0 for $L \sim 9$). As a result of this procedure, we find clear agreement with a $L=6$ transfer for the 3.15 MeV state whereas the complex peak at 3.51 MeV (with a global ratio of ~ 1.2) is excited through a larger L transfer ($L \geq 8$) in addition to the $L=6$ contribution expected at 3.47 MeV. A peak fitting procedure leads to a decomposition into two levels at 3.52 and 3.47 MeV (see Table V) with cross-section ratios in quite good agreement with $L=9$ and $L=6$ attributions, respectively. Indeed, a 9^- state has been observed at the same excitation energy via in beam γ spectroscopy²⁵ but this state has never been observed via transfer reactions up to now. Besides, a recent inelastic electron and proton scattering study²⁶ and nuclear model calculations^{26,27} have proposed that a similar 9^- state in ^{116}Sn arises from a nearly pure $(g_{7/2} \times h_{11/2})$ neutron 2-qp excitation. Furthermore, the states with the configurations

$(g_{7/2} \times h_{11/2})_{9^-}$ and $(g_{7/2} \times 2d_{5/2})_{6^+}$ are predicted to correspond to the most enhanced transitions of the present experiment. The next levels which would be significantly populated are the $J^\pi=7^-$ states corresponding to the $(d_{3/2}$ or $d_{5/2} \times h_{11/2})$ configurations and expected to lie nearby ($E_x \sim 3.4$ MeV). In summary, the sum rule of all the available 6^+ , 7^- , and 9^- states around 3.4 MeV and their calculated relative yields, support the conclusion that the 3.51 MeV peak is indeed a close doublet consisting of the $J^\pi=9^-$ state at 3.52 MeV for the main part and of the weaker $J^\pi=6^+$ level at 3.47 MeV (Table V).

The experimental cross sections at 7_{lab} are listed for each level in Table V. The mean value \bar{N} deduced from the sum rule is equal to 47.5, a value consistent with a rather pure $(g_{7/2} \times h_{11/2})$ configuration of the 9^- state. However, a small fragmentation ($\sim 15\%$) of this state is suggested by the data from one-neutron-pickup experiments,²³ and also by considering the coupling of neutron 2-qp with proton (1 particle-1 hole) configurations as proposed in ^{116}Sn .²⁶ Then a renormalized value of $N \sim 55$ is obtained. The deduced D_0^2 value of ~ 5.7 is quite consistent with the value of ~ 6.6 deduced from the $^{208}\text{Pb}(p,t)$ study (see Sec. III).

The excited states located between 3.8 and 6.3 MeV are rather weakly populated. The small group of states cen-

tered around 4.12 and 4.52 MeV give cross-section ratios which may characterize a $L \geq 8$ transfer. The $(h_{11/2} \times h_{11/2})_{10^+}$ stretched state is indeed expected around 4 MeV, but with a weak cross section (see Table V) as a result of both unfavored transfer structure amplitude and small occupation probability of the $h_{11/2}$ orbital. The global missing $6^+ + 7^- + 9^-$ strength ($\sim 15\%$) would also be exhausted in that same region by the weak coupling states and possibly additional states arising from the mixing with the proton particle-hole configurations.²⁶

2. The $(1V+1D)$ hole structure at 7.3 MeV

Another remarkable feature of the $^{116}\text{Sn}(p,t)^{114}\text{Sn}$ residual energy spectrum (Fig. 2) is the observation of a wide bump centered at 7.3 MeV whereas a similar gross structure has been seen around 8.3 MeV in the study of the $^{116}\text{Sn}(\alpha, ^6\text{He})$ reaction at 218 MeV.¹⁰ This broad structure was first observed around 8 MeV in ^{114}Sn spectra from the $^{116}\text{Sn}(p,t)^{114}\text{Sn}$ reaction at 42 MeV incident energy.^{6,7} The measured angular distribution at 42 MeV does not exhibit a definite L transfer pattern but shows rather a large admixture of many L transfers with no dominant contributions.^{6,7}

Using a simple pairing model, based on the excitation

TABLE V. Summary of the high-spin states populated in ^{114}Sn via the (p,t) reaction at 168 MeV and comparison with previous results.

(p,t) 27.5 MeV ^a		$(\alpha, ^6\text{He})$ 218 MeV ^b		E_x (MeV)	(p,t) 168 MeV (this work)		configuration	$\sigma_{\text{calc}}^{(\mu b)}$ ^d
E_x (MeV)	J^π	E_x (MeV)	J^π		$\sigma_{\text{exp}}^{(\mu b)}$ ^c	J^π		
2.815	5^-			2.85	1.12	$(4^+, 5^-)$		
3.087	(7^-)					(7^-)	$(d_{5/2} \times h_{11/2})_{7^-}$	1.18
3.148	6^+	$\left\{ \begin{array}{c} 3.15 \\ + \\ 3.40 \end{array} \right\}$	6^+	3.15 ± 0.01	4.27	$\left\{ \begin{array}{c} 6^+ \end{array} \right\}$	$(d_{3/2} \times h_{11/2})_{7^-}$	1.23
3.472	6^+			3.47 ± 0.02	2.1	$6^+, (7^-)$	$(g_{7/2} \times 2d_{5/2})_{6^+}$	3.57
				+	+		$(g_{7/2})_{6^+}^{-2}$	0.108
3.515	—			3.52 ± 0.015	6.55	9^-	e	e
				3.96 ± 0.04	0.7	< 8		
				4.16 ± 0.03	1.3	≥ 8	$(g_{7/2} \times h_{11/2})_{9^-}$	6.55
				4.52 ± 0.015	2.34	≥ 8	if $(h_{11/2})_{10^+}^{-2}$	0.52
		$\left\{ \begin{array}{c} \langle 7.45 \rangle \\ + \\ \langle 8.30 \rangle \end{array} \right\}$	$6^+ + (8^+)$	$\langle 7.3 \rangle$	15.5 ^f	8^+	$(g_{9/2} \times g_{7/2})_{8^+}$	17.5
				6^+	$\langle 8.3 \rangle$	or	+	
					(37.5) ^g	(6^+)	$(g_{9/2} \times d_{5/2})_{6^+}$	4.13
						+	$(g_{9/2} \times d_{3/2})_{6^+}$	3.90
						(9^-)	$(g_{9/2} \times 1h_{11/2})_{9^-}$	3.53

^aReference 24.

^bReference 10.

^cExperimental cross sections at $\theta_{\text{lab}} = 7^\circ$.

^dCalculated cross sections at $\theta_{\text{lab}} = 7^\circ$ for the 6^+ , 7^- , 8^+ , and 9^- transitions such as $\sigma_{\text{calc}} = N \sigma_{\text{DWBA}} \times V_j^1 V_j^2$. The occupation number V_j^2 are taken from Ref. 23. The normalization factor $N=47.5$ is deduced assuming that the 6^+ , 7^- , and 9^- summed valence-valence strength is exhausted by the two strongly excited groups at $E_x = 3.15$ MeV and 3.51 MeV. $N \sim 55$ if some fragmentation is taken into account. (See the text.)

^eSame as above.

^fBackground subtracted (see Fig. 2).

^gTotal cross section for the excitation energy slice between 6.3 and 10 MeV.

energy of the 1D, 1V, 1D+1V, and 2D states, the authors of Ref. 28 have proposed that the main contribution to this broad enhancement of cross sections arises from the (1V+1D) hole configurations in the tin isotopes. The deep orbital of interest is the $1g_{9/2}$, located around 5.3 MeV in ^{115}Sn as shown in the previous investigation of the one-neutron-pickup studies.^{21,23} In the reported $^{116}\text{Sn}(\alpha, ^6\text{He})^{114}\text{Sn}$ experiment,¹⁰ it was first suggested that the broad structure may arise from the superposition of two distinct components, one at 7.3 MeV and a stronger one at 8.3 MeV, with a total full width at half maximum (FWHM)= 2.2 ± 0.15 MeV. As nicely demonstrated by the displayed spectra of Fig. 2, the observed differences in the peak position and the shape of the bump from the comparison of the two high incident energy transfer reactions, definitively confirm the previous assumption. The first component, centered at 7.3 MeV, is strongly excited via the (p,t) reaction while the second one located at 8.3 MeV is more enhanced in the $(\alpha, ^6\text{He})$ spectrum and in the (p,t) spectrum taken at 42 MeV incident energy. The measured FWHM from the present (p,t) experiment is of about 1.8 MeV (background subtracted).

From the angular dependence of the bump cross section, measured in the $(\alpha, ^6\text{He})$ reaction, a dominant $L=6$, $J^\pi=6^+$ assignment was proposed. In addition, the small component at 7.3 MeV was better described by adding a $L=8$ component. The $J^\pi=6^+$ contribution is believed to arise mainly from the $(d_{5/2}, d_{3/2}\times g_{9/2})$, (1V+1D) configurations while the 8^+ contribution would be due to the $(g_{7/2}\times g_{9/2})_{8^+}$ (1V+1D) stretched state.

In the present work, the largest DWBA cross section is indeed predicted for this quaspure $(g_{7/2}\times g_{9/2})_{8^+}$ state (see Table V). Furthermore, the ratio of the cross sections at 3.5° and 7.0° for the bump, is consistent with a dominant $L\geq 8$ transfer. These features strongly suggest that the bump observed at 7.3 MeV in the present study is mainly due to the excitation of the $(g_{7/2}\times g_{9/2})_{8^+}$ stretched state while the 6^+ components, more widely spread, contribute to the high-energy tail of the gross structure, giving rise to an asymmetric shape (see Fig. 2). The small occupation probability of the $h_{11/2}$ orbit combined with an unfavored structure amplitude leads to relatively small cross sections for the stretched $(h_{11/2}\times g_{9/2})_{9^-}$ state (see Table V). The expected relative yields of these 8^+ , 6^+ , and 9^- (1V+1D) strengths, from DWBA predictions, are 0.56, 0.33, and 0.11, respectively, while the experimentally extracted cross sections of the bump (background subtracted) (see Fig. 4) exhaust at least $\sim 50\%$ of the full 8^+ , 6^+ , and 9^- strength. This result can be easily understood since about that same amount of the $1g_{9/2}$ deep hole strength is spread over a comparable excitation energy range in ^{115}Sn with a strong concentration (30% over ~ 1 MeV) at 5.3 MeV.^{21,23}

The theoretical predictions on the high-spin 2-qp strength distribution in medium-heavy weight nuclei for the (1V+1D) region are rather scarce. The only calculations available for such high-spin configurations ($J\geq 6$) in ^{114}Sn are reported by Voronov *et al.*²⁹ within the quasiparticle phonon model (QPM). The corresponding

strength distributions are displayed as an inset in Fig. 4. The agreement between theory and experiment is very encouraging since the relative positions of the 8^+ and 6^+ components which are observed in the (p,t) and $(\alpha, ^6\text{He})$ spectra, respectively, are nicely reproduced. Further calculations are however needed, especially for the $(h_{11/2}\times g_{9/2})_{9^-}$, $(h_{11/2}\times p_{1/2}, p_{3/2})_{6^+}$, and $(d_{3/2}\times g_{9/2})_{6^+}$ states which would allow, in particular, a discussion of the asymmetric shape of the (p,t) bump.

We would like to stress that the 2-qp excitations located in the bump region which are strongly excited by means of two-neutron-pickup reactions are not populated in proton or electron inelastic scattering on Sn targets or proton stripping reactions on In nuclei.²⁶ This gives further support to the conclusion that they arise from quaspure neutron 2-qp excitations. Beyond this enhanced bump no evidence is found, at least up to about 17 MeV excitation energy, for any significant concentration of high-spin two-neutron deep-hole strengths, whereas from energy considerations and pairing model assumptions, these configurations should lie around 12 MeV in ^{114}Sn .

V. SUMMARY AND CONCLUSIONS

The $^{208}\text{Pb}(p,t)^{206}\text{Pb}$ and $^{116}\text{Sn}(p,t)^{114}\text{Sn}$ reactions have been investigated for the first time at high incident energy (168 MeV). The kinematical conditions have allowed a strong excitation of the high-spin stretched two-neutron-hole states ($J\geq 6$) in both residual nuclei. Among them the two-nucleon structure amplitudes favor the

$$[(l_1 + \frac{1}{2}) \times (l_2 - \frac{1}{2})]_{J_{\max}}$$

spin coupling as compared to the $(jj)J_{\max}$ or

$$[(l_1 \pm \frac{1}{2}) \times (l_2 \pm \frac{1}{2})]$$

combinations. This feature is clearly established in the $^{208}\text{Pb}(p,t)$ reaction where the dominant stretched state is the 11^- level from the $(h_{9/2}\times i_{13/2})$ configuration rather than the 12^+ level from the $(i_{13/2})^{-2}$ one.

The data have been analyzed in the framework of the LZR-DWBA theory of nuclear reactions. From a sum-rule analysis based on the 9^- high-spin transitions, a reliable ZRNC D_0^2 has been deduced, namely $D_0^2 \sim 6.6$ ($10^4 \text{ fm}^3 \text{ MeV}^2$) from the $^{208}\text{Pb}(p,t)^{206}\text{Pb}$ study and $D_0^2 \sim 5.7$ ($10^4 \text{ fm}^3 \text{ MeV}^2$) from the $^{116}\text{Sn}(p,t)^{114}\text{Sn}$ experiment. Using different assumptions in the ^{206}Pb analysis, the D_0^2 values might range from a minimum value of ~ 4.2 to a maximum value of ~ 8.3 . The D_0^2 quantities are thus found to be much smaller than the commonly adopted value of $D_0^2=22$ ($10^4 \text{ fm}^3 \text{ MeV}^2$) at lower incident energy.

The relative enhancement factors (ϵ_R), for the $J^\pi=9_1^-$, $(f_{5/2}\times i_{13/2})$ reference state ($\epsilon_{9_1^-}=1$), have been deduced assuming pure two-neutron-hole configurations. We have shown that even a slight configuration admixture ($\sim 5\text{--}10\%$) in the wave function of an unfavored state may affect the corresponding predicted cross section considerably due to large interference effects between the amplitudes of the two-nucleon configurations. The comple-

mentary aspect of both the (p, t) and ($\alpha, {}^6\text{He}$) reactions performed at high incident energy has been pointed out, and the detailed comparison of the two reactions yields a more consistent interpretation of the data.

In ${}^{206}\text{Pb}$, all the high-spin stretched states ($J \geq 6$) have been unambiguously identified, in particular the $(i_{13/2} \times h_{9/2})_{11-}$ level at $E_x = 5.39$ MeV state and the $(i_{13/2})_{12+}^{-2}$ level at 4.0 MeV. A fairly consistent description of the main transitions observed between $E_x = 2.2$ and 6.1 MeV is achieved by taking into account the known fragmentation of each single hole state in ${}^{207}\text{Pb}$, with about 25% of the (1V+1V) cross section being pushed up above 6.7 MeV. Weak structures are observed up to ~ 7.9 MeV which could be attributed to a small part of the high-spin missing strength which appears mostly embedded into the continuum. No significant concentration of (1V+1D $h_{11/2}$) nor of 2D hole strengths has been observed up to $E_x \sim 25$ MeV though they are expected around 10 and 17 MeV, respectively.

In ${}^{114}\text{Sn}$, neutron 2-qp excitations are strongly exhibited at 3.15 and 3.51 MeV. The previous 6^+ attribution to the 3.15 MeV state is confirmed and the $(g_{7/2} \times h_{11/2})_{9-}$ stretched state is identified for the first time at 3.52 MeV in the present experiment. This 9^- component is observed as the main contribution of a doublet which also includes the known 6^+ state at $E_x = 3.47$ MeV. According to the small measured fragmentation of neutron single hole strengths in ${}^{115}\text{Sn}$, most of the available 6^+ , 7^- , and 9^- strengths would be exhausted in the clustering of levels located between $E_x \sim 3$ and 3.7 MeV. However, it would be interesting to further study the behavior of such 9^- stretched states in other tin isotopes and nearby nuclei, as well as the coupling between neutron 2-qp configurations and proton (1p-1h) configurations recently predicted.²⁶

The broad bump observed in the present ${}^{116}\text{Sn}(p, t)$ reaction has its maximum at $E_x = 7.3$ MeV instead of at 8.3 MeV as observed in the previous works. This result definitively confirms the existence of two high-spin components in that (1V+1D) structure. The first one is believed to arise mainly from the $(g_{7/2} \times g_{9/2})_{8+}$ state whereas the second one, which also exhibits a larger width, is mainly due to the excitation of the $(d_{5/2,3/2} \times g_{9/2})_{6+}$ states. The search for a significant

concentration of the (2D) hole strength has been unsuccessful up to ~ 17 MeV excitation energy, though expected around 11–12 MeV.

To conclude we would like to emphasize the very different features of the two-neutron-hole distributions in ${}^{114}\text{Sn}$ and ${}^{206}\text{Pb}$.

The main (1V+1V) high-spin states are concentrated over less than 1 MeV in ${}^{114}\text{Sn}$, whereas they are distributed over about 4 MeV in ${}^{206}\text{Pb}$. The ${}^{114}\text{Sn}$ spectra exhibit a strong concentration of the (1V+1D) high-spin strengths, which is not the case for the ${}^{206}\text{Pb}$ spectra. These features are qualitatively understood by considering each related single hole (1V) and (1D) fragmentation independently. For example the (1V+1D $g_{9/2}$) gross structure around 7.3 MeV in ${}^{114}\text{Sn}$ exhibits the fingerprint of the strong concentration of the 1D $g_{9/2}$ hole strength in the dominant fragment at 5.3 MeV in ${}^{115}\text{Sn}$, whereas the corresponding 1D $h_{11/2}$ hole strength is much more widely spread in ${}^{207}\text{Pb}$ and lies at higher excitation energy (~ 8.3 MeV).

The present experimental study of two-neutron-hole fragmentation in ${}^{206}\text{Pb}$ and ${}^{114}\text{Sn}$ might indicate that this fragmentation is globally slightly smaller than from a crude estimation based on these related one-hole fragmentations as previously measured. Further data on different nuclei would help to settle this point, as well as theoretical predictions.

There is a great lack of calculated two-neutron-hole strength functions in medium-heavy nuclei especially for high-spin stretched states with (1V+1D) and (2D) configurations. The damping of such simple modes of nuclear excitations would need to be investigated within the same framework as the one employed to predict the single-particle response function,³⁰ where the surface vibrations have been found to play a dominant role. Consistent calculations of the neutron 2-qp state spreading with increasing excitation energy, in connection with the relevant single-particle response functions are highly desirable.

The authors would like to thank the synchrocyclotron crew for the good running of the accelerator and G. Chesneau for his help with the wire chamber operation and the electronic setup.

¹S. Galès, in Lectures at the International School on Nuclear Structure Alhusta, URSS, 1985, edited by V. G. Soloviev and Y. P. Popov (unpublished), p. 51, and references therein.

²H. Langevin-Joliot, in Lectures at the XIV Mazurian School, Lake Mikolajki, Poland, 1983, edited by Z. Wilhelmi and M. Kicińska-Habior, Vol. 8 of Nuclear Sciences Research, Conferences Series (1986), p. 101; Orsay Internal Report IPNO-DRE/83-36.

³M. Matoba, K. Tsuji, K. Marubayashi, T. Shintake, K. Ohba, and T. Nomiya, Phys. Rev. C **27**, 2598 (1983)

⁴J. R. Shepard, R. E. Anderson, J. J. Kraushaar, R. A. Ristinen, J. R. Comfort, N. S. P. King, A. Bacher, and W. W. Jacobs,

Nucl. Phys. **A322**, 92 (1979).

⁵G. M. Crawley, S. Galès, D. Weber, B. Zwieglinski, W. Benenson, D. Friesel, A. Bacher, and B. M. Spicer, Phys. Rev. C **22**, 316 (1980).

⁶G. M. Crawley, W. Benenson, D. Weber, and B. Zwieglinski, Phys. Rev. Lett. **39**, 1451 (1977).

⁷G. M. Crawley, W. Benenson, G. Bertch, S. Galès, D. Weber, and B. Zwieglinski, Phys. Rev. C **23**, 589 (1981).

⁸N. K. Glendenning, At. Data Nucl. Data Tables **16**, 1 (1973).

⁹T. Kurihara, S. Kubono, M. Sekiguchi, M. H. Tanaka, M. Sakai, Y. Fujita, M. Fujiwara, and E. Gerlic, Nucl. Phys. **A457**, 45 (1986).

- ¹⁰E. Gerlic, J. Guillot, H. Langevin-Joliot, S. Galès, M. Sakai, J. Van de Wiele, G. Duhamel, and G. Perrin, *Phys. Lett.* **117B**, 20 (1982).
- ¹¹M. Morlet and A. Willis, IPN Orsay Internal Report IPNO-PhN/79-15, 1979; J. Guillot, 3rd Cycle thesis, Orsay, 1982.
- ¹²M. Takahashi, T. Murakami, S. Morita, H. Orihara, Y. Ishizaki, and H. Yamaguchi, *Phys. Rev. C* **27**, 1454 (1983), and references therein.
- ¹³H. Orihara, Y. Ishizaki, G. F. Trentelman, M. Kanazawa, K. Abe, and H. Yamaguchi, *Phys. Rev. C* **9**, 266 (1974).
- ¹⁴I. Kumabe, M. Hyakutake, K. Yuasa, T. Yamagata, S. Kishimoto, T. Komatsuzaki, Y. Ishizaki, T. Tohei, and T. Nakagawa, in *Proceedings of the RCNP International Symposium on Highly Excited States in Nuclear Reactions*, edited by H. Ikegami and M. Muruoka (RCNP, Osaka, Japan, 1980), p. 644.
- ¹⁵C. Djalali, 3rd Cycle thesis, Orsay, 1981.
- ¹⁶A. Djaloeis, J. P. Didelez, A. Galonsky, and W. Oelert, *Nucl. Phys.* **A306**, 221 (1978).
- ¹⁷J. Guillot *et al.*, in *Contributions to the International Symposium HESANS*, Orsay, 1983, edited by N. Marly and N. Van Giai (unpublished), p. 14; Orsay IPN Annual Report 1983; and private communication.
- ¹⁸P. D. Kunz, G. N. Hassold, J. J. Kraushaar, P. A. Smith, and E. F. Gibson, *Nucl. Phys.* **A367**, 13 (1981).
- ¹⁹T. T. S. Kuo and G. H. Herling, Naval Research Memorandum Report 2258, 1971, unpublished.
- ²⁰J. Guillot, J. Van de Wiele, H. Langevin-Joliot, E. Gerlic, J. P. Didelez, G. Duhamel, G. Perrin, M. Buenerd, and J. Chauvin, *Phys. Rev. C* **21**, 879 (1980); J. Van de Wiele, E. Gerlic, H. Langevin-Joliot, and G. Duhamel, *Nucl. Phys.* **A297**, 67 (1978).
- ²¹H. Langevin-Joliot, E. Gerlic, J. Guillot, M. Sakai, J. Van de Wiele, A. Devaux, P. Force, and G. Landaud, *Phys. Lett.* **114B**, 103 (1982), and references therein.
- ²²*Nucl. Data Sheets*, **26**, 145 (1979).
- ²³E. Gerlic, G. Berrier-Ronsin, G. Duhamel, S. Galès, E. Hourani, H. Langevin-Joliot, M. Vergnes, and J. Van de Wiele, *Phys. Rev. C* **21**, 124 (1980).
- ²⁴P. J. Blankert, Ph.D. thesis, Vrije Universiteit, Amsterdam, 1979.
- ²⁵A. Van Poelgeest, J. Bron, W. H. A. Hesselink, K. Allaart, J. J. A. Zalmstra, M. J. Uitzinger, and H. Verheul, *Nucl. Phys.* **A346**, 70 (1980).
- ²⁶S. Y. van der Werf, N. Blasi, M. N. Harakeh, G. Wenes, A. D. Bacher, G. T. Emery, C. W. Glover, W. P. Jones, H. J. Karwowski, H. Nann, C. Olmer, P. Den Heijer, C. W. De Jagger, H. De Vries, J. Ryckebusch, and M. Waroquier, *Phys. Lett.* **166B**, 372 (1986); M. Waroquier, J. Ryckebusch, J. Moreau, K. Heyde, N. Blasi, S. Y. van der Werf, and G. Wenes, *Phys. Rep.* **148**(5), 249 (1987).
- ²⁷G. Bonsignori, M. Savoia, K. Allaart, A. Van Egmond, and G. Te Velde, *Nucl. Phys.* **A432**, 389 (1985).
- ²⁸G. M. Crawley, in *Proceedings of the International Conference on Structure of Medium-Heavy Nuclei, Rhodos, 1979*, edited by the "Demokritos" Tandem Accelerator Group (The Institute of Physics, Bristol, 1980), p. 127; *Proceedings of International Symposium on Highly Excited States*, edited by H. Ikegami and M. Muruoka (RCNP, Osaka, 1980), p. 590.
- ²⁹V. V. Voronov, in *Contributions to the International Symposium HESANS*, Orsay, 1983, edited by N. Marty and N. van Giai (unpublished), p. 21; V. G. Soloviev, O. Stoyanov, and V. V. Voronov, *Nucl. Phys.* **A370**, 13 (1981).
- ³⁰F. Zardi, P. F. Bortignon, E. Maglione, and A. Vitturi, in *Proceedings of the XXI International Winter Meeting on Nuclear Physics, Bormio, 1983*, edited by I. Iori (Ricerca Scientifica ed educazione permanente, Milano, 1983), p. 461; G. F. Bertsch, P. F. Bortignon, and R. A. Broglia, *Rev. Mod. Phys.* **55**, 287 (1983).